AD-A240 559

②

BRL

GENERALIZED FINITE ELEMENT GAP MODEL

DTIC
ELECTE
SEP 19 1991
S D

ADAM R. ZAK
ZAK TECHNOLOGIES, INC.

AUGUST 1991

91-10777

U.S. ARMY LABORATORY COMMAND

BALLISTIC RESEARCH LABORATORY
ABERDEEN PROVING GROUND, MARYLAND

NOTICES

REPORT DOCUMENTATION PAGE

Form Approved
OMB No. 0704-0188

1. AGENCY USE ONLY *(Leave blank)*	2. REPORT DATE August 1991	3. REPORT TYPE AND DATES COVERED Final, Apr 86 - Jan 87

4. TITLE AND SUBTITLE

Generalized Finite Element Gap Model

5. FUNDING NUMBERS

PR: 1L162618AH80

6. AUTHOR(S)

Adam R. Zak

7. PERFORMING ORGANIZATION NAME(S) AND ADDRESS(ES)

Zak Technologies, Inc.
2310 Belmore Drive
Champaign, IL 61821

8. PERFORMING ORGANIZATION REPORT NUMBER

9. SPONSORING / MONITORING AGENCY NAME(S) AND ADDRESS(ES)

U.S. Army Ballistic Research Laboratory
ATTN: SLCBR-DD-T
Aberdeen Proving Ground, MD 21005-5066

10. SPONSORING / MONITORING AGENCY REPORT NUMBER

BRL-CR-670

11. SUPPLEMENTARY NOTES

This work was performed under the auspices of the U.S. Army Ballistic Research Laboratory by Zak Technologies, Inc., under Contract No. DAAA15-85-C-0021. The Contracting Officer's Representative is Dr. Bruce P. Burns, U.S. Army Ballistic Research Laboratory, ATTN: SLCBR-IB-M, Aberdeen Proving Ground, MD 21005-5066

12a. DISTRIBUTION / AVAILABILITY STATEMENT

Approved for public release; distribution is unlimited.

12b. DISTRIBUTION CODE

13. ABSTRACT *(Maximum 200 words)*

This report covers topics related to the application of finite element methods. If specifically talks about the codes named SAGA, SAAC, SAAC3, and SAAC3X. Included are examples of generalized input.

14. SUBJECT TERMS

loading; stiffness; gaps; finite element; models; computer codes

15. NUMBER OF PAGES

50

16. PRICE CODE

17. SECURITY CLASSIFICATION OF REPORT	18. SECURITY CLASSIFICATION OF THIS PAGE	19. SECURITY CLASSIFICATION OF ABSTRACT	20. LIMITATION OF ABSTRACT
UNCLASSIFIED	UNCLASSIFIED	UNCLASSIFIED	SAR

NSN 7540-01-280-5500

Standard Form 298 (Rev 2-89)
Prescribed by ANSI Std 239-18
298-102

INTENTIONALLY LEFT BLANK.

TABLE OF CONTENTS

iii

INTENTIONALLY LEFT BLANK.

LIST OF FIGURES

INTENTIONALLY LEFT BLANK.

1. INTRODUCTION

This report covers a number of topics related to the application of finite element methods to ballistic structural problems. All of these topics are extensions and modifications of finite element formulations and computer codes previously developed in this technical area.

The first topic to be discussed involves an extension of so-called gap element formulation (Zak 1984). In a previous study, a finite element model was developed which can handle material contact problems inside of a structure. This occurs when the unloaded structure contains small gaps which can close when the load is applied. The contact of the adjacent portions of the structure leads to a nonlinear response. The finite element model previously developed for this problem makes use of so-called gap elements. In this approach, the gaps are modelled by these elements which simulate the nonlinear, physical phenomena of material contact. This finite element model was incorporated into a three-dimensional, axisymmetric program call SAGA. In this application, the gaps were allowed to exist either in the I or J directions in the I-J plane of the finite element grid. The restriction of the gap geometry to be in either one of these directions placed a constraint on the type of geometries which could be handled. For example, if the gap made a number of sharp changes in direction, the original formulation would not be applicable. Consequently, it was decided to develop a new computer code for the contact problem in which this restriction would be removed. The development of this code will be described in this report.

The second topic of this report will deal with another modification to the original gap element formulation (Zak 1984). In the original finite element formulation, a rather simplified model was employed to represent material slip after gap closure. If the closure of the gap occurs during the loading cycle, the gap surfaces will not move relative to each other in the direction normal to the gap. However, in the tangential direction, relative motion is possible. In the original gap element model, the tangential forces were kept constant. The objective of the modified model is to make these tangential forces proportional to the normal compressive force across the gap. This feature was added to the new gap element code which allows for combined I-J directions of the gap.

1

The third topic to be dealt with in this report consists of adding rate-dependent plasticity to the gap computer code (Drysdale and Zak 1983). In a previous study, a material model was developed in which the yield condition is a function of plastic strain rate. This model was applied to finite element theory and incorporated into a computer program called SANX (Zak, Craddock, and Drysdale 1979). The present objective was to use this material model in the gap element computer code. In addition, some further improvements to this model were incorporated so as to eliminate numerical oscillations which occurred in SANX when abrupt changes were made in the loading conditions. For example, one interesting situation consisted of a slender structural member subject to torsional load which was held constant at yield and then followed by constant normal strain rate. This loading produces large discontinuities and, consequently, numerical oscillations. Reformulation of the computational procedure has eliminated numerical oscillations.

The fourth and the last topic to be discussed involves some preliminary investigation of code combinations. During a number of past investigations, many different but related finite element codes have been developed for ballistic applications. The purpose of the codes is to handle a number of different configurations, material properties, and loading conditions. During the present investigation, some preliminary work was done on the feasibility of combining these codes so that advantage can be taken of common features such as the finite element grid generation and other input preparation.

2. EXTENDED GAP GEOMETRY

2.1 Introduction to SAGA Program. The original gap element computer program is called SAAC (Zak 1984). The starting point for the development of this program was the SAGA program. Before describing the SAAC program and its extension in this investigation, it is useful to briefly review the SAGA code and its application.

Originally, the SAGA program was developed for elastic materials. The elastic SAGA itself is an extension of an axisymmetric code called SAAS. The SAAS is a basic finite element program with two degrees of freedom at each node. Some time ago, it was useful to extend this code to an axisymmetric code with three degrees of freedom at each node. This new code was denoted as SAGA. The motivation for this new code was to permit solution of

2

problems containing torsional loads and problems involving orthotropic materials where the axis of orthotropy is out of the meridian plane.

Before modifying the SAGA program to incorporate the gap element model, it was necessary to develop an elastic-plastic version called SAGAEP. This program handles the problem by incremental solution. Both the loads and the material properties are varied incrementally. The incremental nature of the SAGAEP program was necessary since the gap program SAAC is nonlinear even if the material properties are elastic. The nonlinear nature arises from the gap contact phenomena. However, one of the original requirements in the SAAC development was to incorporate plasticity.

2.2 Introduction to SAAC Program. Since the original SAAC program forms the basis for three aspects of this investigation, it is necessary to describe briefly the main features of the gap element model and its incorporation into the computer code.

The basic idea of gap elements is that they simulate the gap before closure and after closure. The gap element material properties are altered to simulate material contact. This is done by originally assigning very low stiffness properties to the element. If contact occurs, certain of the stiffness properties are changed to make the element very stiff in the direction perpendicular to the gap direction.

The gap finite element model can be described by referring to Figure 1 through 8. Figure 9 shows the flow chart for the program SAAC. The basic ideas of the gap element model are first developed with reference to the I-J grid. The I-J coordinate system will locate elements and nodal points. To illustrate how nodal points are located, take a typical element in an I-J grid (Figure 1). The element has nodal point IX(N,1) located at the corner that lies closest to the origin. The remaining three nodal points IX(N,2), IX(N,3), and IX(N,4) are obtained by moving in the counterclockwise direction around the element. The direction of the gap depends on an input parameter called the principal gap direction. As an example, if the principal gap direction parameter is chosen to be equal to 1; then, the gap direction will be parallel to the J-axis while the direction of closure will be parallel to the I-axis (Figure 2). If the principal gap direction is set to 2, the direction of the gap will be parallel to the I-axis while the gap closure will be in the J-axis direction (Figure 3). In the present model and the

3

program SAAC, there is only one choice available for the gap direction parameter. For example, if the parameter is chosen to be 1, all gap elements will have that direction.

The gap direction will determine which node points will be opposite one another along the gap. This information is important for reasons that will be best understood from the following discussion. First, the program must know which node points to pair and then test for contact; and secondly, when contact is established, the nodal point pairs will be used to properly modify gap element material properties. Referring to Figure 2, if the principal gap direction is set to 1, then the two nodal pairs for the element are (IX[N,1], IX[N,2]) and (IX[N,3], IX[N,4]). Similarly, for a principal gap direction of 2, the two pairs are (IX[N,1], IX[N,4]) and (IX[N,2], IX[N,3]).

The third geometric parameter has to do with the orientation of the gap element relative to the R-Z axes. This orientation will be used to transform nodal positions and nodal displacements into a coordinate system where one axis coincides with the direction of the gap, while the other axis coincides with the direction of the closure. The second use of the gap orientation will insure that gap material properties will only stiffen in the direction of closure once contact is established.

Once the principal gap direction is set, the angle of the gap can be calculated. This angle is defined in a manner indicated by Figure 4. As an example, take a typical element with a principal gap direction of 1 and nodal points $I1$, $I2$, $I3$, and $I4$ [equal to IX(N,1), IX(N,2), IX(N,3), and IX(N,4) respectively]. The angle β will be calculated by first producing a "mean" line through the element (Figure 5). The coordinates of points A and B are, respectively, as follows:

$$R_A, Z_A = \frac{R(I1) + R(I4)}{2} , \frac{Z(I1) + Z(I4)}{2} , \tag{1}$$

$$R_B, Z_B = \frac{R(I2) + R(I3)}{2} , \frac{Z(I2) + Z(I3)}{2} . \tag{2}$$

4

Using the expressions (Equations 1 and 2), the angle β can be calculated by using the following:

$$\beta = ARCtan \, \frac{(R_B - R_A)}{(Z_B - Z_A)} \, .$$

(3)

This definition of β will have coordinate axis N coincident with the direction of closure and coordinate axis T coincident with the gap direction.

If the principal gap direction is equal to 2, the angles (Equations 1 and 2) are changed by pairing off points $I1$ with $I2$ and $I3$ with $I4$. Otherwise, the calculation for β is the same as in Equation 4. The establishment of the nodal pairs also permits the calculation of the gap size at each end of the element. The significance of the gap size is that it is later used to check if gap closure occurs. In the SAAC program, the geometrical properties of gap, including the orientation and the gap size, are calculated in the Subroutine GAPANG shown in Figure 9.

The solution of the structural problem is performed incrementally. The external load is divided into load steps. At each load step, the solution checks for closure at each set of nodal pairs for each gap element. The closure is determined by comparing the normal displacement components with the original gap size. Determining whether or not opposing node points have contacted is done by first transforming nodal displacements and nodal positions into the N, T, S coordinate system. The coordinates N and T are given in Figure 4, and S is defined to be orthogonal to N and T. Transformation from the R, Z, θ coordinate system to the N, T, S coordinate system is of the following form:

$$\begin{Bmatrix} U_N \\ U_T \\ U_S \end{Bmatrix} = [T] \begin{Bmatrix} U_R \\ U_Z \\ U_\theta \end{Bmatrix} ,$$

(4)

where U_R, U_Z, and U_θ are the nodal displacements in the R, Z, and θ directions, respectively.

The transformation matrix [T] is as follows:

$$[T] = \begin{bmatrix} SIN\beta & COS\beta & 0 \\ -COS\beta & SIN\beta & 0 \\ 0 & 0 & 1.0 \end{bmatrix} , \tag{5}$$

where the angle β is defined by Equation 3. As can be seen in Equation 5, the coordinate axes θ and S will always coincide in this transformation.

The transformation of nodal positions is similar to the transformation of nodal displacements. This transformation is of the following form:

$$\begin{Bmatrix} P_N \\ P_T \end{Bmatrix} = [T'] \begin{Bmatrix} P_R \\ P_Z \end{Bmatrix} , \tag{6}$$

where P_R and P_Z are the nodal positions in the R and Z directions, respectively. P_N and P_T are the nodal positions in the N and T directions, respectively. The transformation matrix [T'] is as follows:

$$[T'] = \begin{bmatrix} SIN\beta & COS\beta \\ -COS\beta & SIN\beta \end{bmatrix} . \tag{7}$$

Since we are dealing with axisymmetric elements, the U_θ does not affect gap closure. The second step in the test for contact involves updating nodal positions in the N direction. The updating occurs at the end of every load step. This procedure is applied to each nodal pair for each gap element. The new relative position of the nodal pairs determines the gap closure. When the gap is closed, no further relative motion in the normal gap direction will be allowed. When real gaps close, the two opposing material faces will never overlap one

6

another. For an effective simulation of real gaps, this behavior must be duplicated in the finite element model. It is conceivable that a nodal pair that is not contacting at the end of a given load step can be overlapping at the end of the next load step. This can occur because the program only checks for contact at discrete load intervals and not continuously. The analysis handles the problem of overlapping by splitting load steps. The first step in this process takes all the nodal pairs that are overlapping at the end of a given load step and calculates a factor for each one that depends on the degree of overlap. This procedure works something like this: When a particular load step causes a nodal pair closure and an overlap, the load step is modified. For example, suppose a load step causes nodal pair relative displacement twice as large as necessary to just close the gap. Then this load step is modified by a factor of one-half, and the analysis is repeated for the new, smaller load. Testing for contact and the calculation of load factors occur in Subroutine TEST. The Subroutine TEST is called from Subroutine SOLV after nodal displacements have been calculated. An assumption is made to the load factor analysis to reduce execution time. The assumption is that the contact condition of nodal pairs is determined by the original load step and not by the reduced load step. As an example of this, if a given number of nodal pairs are overlapping at the end of a load step, the program will then assume that these nodal pairs will remain in contact even though the load step will be reduced. An advantage of this assumption is that original load steps are only split once. A disadvantage, however, is that the program might predict gap closure at a different load as compared to a real structure with the same configuration. This problem is minimized by keeping load steps small.

After gap closure has been established, the nodal pairs involved will not move relative to each other in the N direction. Unloading, of course, could separate the gap, and program SAAC can handle this possibility. The gap element simulates the contact situation by changing certain stiffness properties of the element. This is not done by changing the material properties but rather by directly changing the stiffness matrix of the gap element.

The global coordinates which the SAAC program uses are the cylindrical coordinates R, Z, and θ. Consequently, the stiffness matrix for all elements is assembled in these coordinates. However, in order to simulate the gap closure, it is necessary to change the element stiffness in the N, T, S coordinate system. The element stiffness matrices in the SAGA and the SAAC

7

programs represent 12 degrees of freedom. Suppose the stiffness matrix in the N, T, S system is represented by the following:

$$[S] = [S_{ij}]_{\substack{i=1,12 \\ j=1,12}} . \tag{8}$$

Before contact, the material properties of the element are chosen to be very soft relative to the structural material surrounding the gap. When the stiffness matrix (Equation 8) is calculated for the gap element, the stiffness coefficients S_{ij} will be small relative to the adjacent structure. For numerical reasons, the material properties cannot be identically zero. When contact is established, the stiffness coefficients in the N, T, S system are modified to simulate the fact that two of the nodal points will move together. This is achieved by increasing the numerical size of certain of the stiffness coefficients. Theoretically, the increasing value of these coefficients could be infinite; however, it has been found that this leads to numerical difficulties. Consequently, the program SAAC increases these coefficients so that they are approximately two magnitudes larger than similar coefficients for adjacent structural materials.

The procedure of changing the stiffness and simulating contact across the gap can be illustrated as follows.

A gap element has four different contact states for each value of the principal gap direction. Consider an element with a principal gap direction of 1 and opposing nodal pairs (1,2) and (3,4) (Figure 7). The following four contact states are possible:

(1) State No. 1 - both node pairs not contacting

(2) State No. 2 - (1,2) contacting; (3,4) not contacting

(3) State No. 3 - (1,2) not contacting; (3,4) contacting

(4) State No. 4 - both nodal pairs contacting.

The gap element stiffness matrix is modified differently for each of the four states. The proper modification of the element stiffness matrix is as follows:

(1) State No. 1 - all matrix elements remain unchanged and small

(2) State No. 2 - set $S_{1,1} = S_{4,4} = -S_{1,4} = -S_{4,1}$ = large number

(3) State No. 3 - set $S_{7,7} = S_{10,10} = -S_{7,10} = -S_{10,7}$ = large number

(4) State No. 4 - set $S_{1,1} = S_{4,4} = S_{7,7} = S_{10,10} = -S_{\cdot} = -S_{4,1} = -S_{7,10} = -S'_{10,7}$
= large number.

If the principal gap direction of the element is equal to 2, the gap element stiffness matrix modification will be similar to that shown previously. However, different stiffness coefficients will be changed as indicated by appropriate degrees of freedom for the nodal pairs.

After modification of the stiffness coefficients in the N, T, S coordinate system, the stiffness matrix is transformed into the cylindrical coordinates. The matrix transformation procedure is given by the following:

$$[K] = [T]^T [S] [T] , \qquad (9)$$

where $[S]$ and $[K]$ are the element stiffness matrices in the N, T, S and R, Z, θ coordinate systems, respectively. The transformation matrix $[T]$ is as follows:

$$[T] = \begin{bmatrix} [t] & & & \\ & [t] & & \\ & & [t] & \\ & & & [t] \end{bmatrix}, \qquad (10)$$

where $[t]$ is given by the following:

$$[t] = \begin{bmatrix} SIN\beta & -COS\beta & 0 \\ COS\beta & SIN\beta & 0 \\ 0 & 0 & 1.0 \end{bmatrix}. \qquad (11)$$

9

In the computer program SAAC, the modification of the gap element stiffness matrix and the coordinate transformation are performed in Subroutine RETRANS as shown in Figure 9.

2.3 Extended General Gap Model. The program SAAC, with the gap element model described previously, forms the starting point for a modified program called SAAC2. This program contains the same basic ideas as SAAC but allows for a general gap configuration. This configuration permits the gap orientations to exist in I and J directions simultaneously. To illustrate this, consider a corner gap in the I and J coordinates as shown in Figure 10. This figure shows three gap elements. Element No. 1 is in the I direction; element No. 2. is in the J direction and the gap element, No. 3, is a corner gap element. For these gaps for which this model is designed, the corner element represents a very small volume of the structure and, therefore, is of negligible contribution. Consequently, in the analysis of SAAC2 corner gap elements such as No. 3 in Figure 10, always retain constant, low stiffness.

The program SAAC2 retains the same arrangement as SAAC and, therefore, has the same flow chart as shown in Figure 9. The basic change in the new model is to allow each element to possess its own direction parameter. This is achieved by adding this parameter to material block input cards. For normal elements, not gap, this parameter is left blank on the input and is ignored.

In order to create program SAAC2 from SAAC, changes have been made in the following parts of the program: MAIN, GAPANG, POINTS, SOLVE, and STIFF.

In Subroutine POINTS, one material block parameter IJDIR(M) is read in for each block. Using this block parameter, an element parameter IG(N) is set up for each element in the structure. As mentioned before, this parameter is automatically taken equal to zero if no input in the material block is entered. This applies to nongap elements. In the original SAAC program, there was only one gap direction parameter—LGAP. This parameter has been retained in SAAC2 problem; however, it is continuously reset for each individual element.

The input instructions for SAAC2 are described in Appendix A. These instructions can also be used for SAAC since the differences are small; and when these differences occur, they are indicated.

10

The program SAAC2 was checked out on a number of test examples. One of the initial checks performed was to compare numerical answers with those from SAAC for one-directional gaps. A number of examples for SAAC were described in the previous report (Zak 1984).

3. GAP MODEL INCLUDING SLIP

3.1 Background and Objectives. In the original study which resulted in the development of the SAAC program (Zak 1984), a preliminary attempt was made to account for material slip forces after the gap was closed. As a result of this effort, a separate version of the program, called SAACFR, was developed which attempted to include slip forces after material contact was achieved. This model was rather simple and was designed only to establish the feasibility of including such effects in the gap element model. One of the objectives of the present study was to develop a more comprehensive slip model which would be more realistic. Before describing the new slip model, it is useful to review briefly the slip model in the original SAACFR program.

In the original SAAC program, no allowance was made for the tangential forces due to material slip after gap closure was achieved. In order to investigate the relative effect of this phenomena, a simple slip model was introduced. The main features of this model are as follows. The model introduces frictional forces which modify the gap stiffness model. The effects of friction are related to the stiffness in the direction of closure. This relationship is made through the use of a frictional coefficient. As an example, if nodal pair (1,2) in an element is contacting, then the following relationships will model friction:

$$S_{2,2} = S_{5,5} = -S_{5,2} = -S_{2,5} = \mu S_{1,1}, \tag{12}$$

$$S_{3,3} = S_{6,6} = -S_{3,6} = -S_{6,3} = \mu S_{1,1}, \tag{13}$$

where μ is a frictional coefficient or simply a proportionality constant between the stiffness coefficients perpendicular to the gap and in the tangential directions. The two normal degrees of freedom are 1 and 4 and, therefore, the four tangential degrees of freedom are 2, 3, and 5, 6. By examining Equations 12 and 13, it can be seen that they relate the tangential

11

stiffness to the normal stiffness after gap closure. In that sense, this modification does restrict the tangential motion; however, it does not fully represent what is normally considered as a frictional behavior. In spite of the limitations of this model, it was useful to examine the relative effect of the slip on the response of a number of test examples. Equations 12 and 13 can be extended easily to nodal pair (3,4). If the nodal pairs are (2,3) and (1,4), similar modified relations can be obtained. The SAACFR program, since it is an extension of SAAC code, automatically determines the nodal pairs and applies the tangential correction as illustrated by Equations 12 and 13. In the test examples executed, the value of frictional coefficient μ had to be estimated based on some reasonable, preliminary estimates.

The modification of stiffness and the friction analysis are both done in Subroutine RETRANS. This change of gap material properties takes place in the N, T, S coordinate system and afterwards is transformed back in the R, Z, θ system.

3.2 Extended Slip Model. As pointed out, the original slip model was designed to be preliminary and did not possess properties which normally are associated with frictional phenomenon of sliding surfaces. The new model which has been developed attempts to overcome these objectives.

The force in slip phenomena is represented by Colomb friction. This can be illustrated by force-displacement relation as shown in Figure 11. Up to a certain point, the force and displacement are linearly related and after certain value of force is exceeded, the force will remain reasonably constant. It can be seen from Figure 11 that the forces involved in the slip phenomena have approximately the same behavior as an elastic perfectly plastic stress-strain relation. In an elastic perfectly plastic response, the stress at which the stress-strain curve becomes flat is known as the yield stress. In the case of the frictional phenomena, the yield stress would correspond to the force at which the force displacement becomes flat. However, unlike in the yield phenomena where yield stress is relatively constant, the value of force where the curve becomes flat (Figure 11) depends on the normal forces. Consequently, the slip phenomena can be modeled on a basis of an analogy with elastic-plastic response where the yield stress becomes a function of normal loads to the direction of the gap. This approach has been taken in the development of an improved slip model.

12

The modified slip model involves the modification of certain of the stiffness coefficients in the gap element. Consider now the modification of Equations 12 and 13 for nodal pair (1,2).

$$S_{2,2} = S_{5,5} = -S_{5,2} = -S_{2,5} = S,$$ (14)

$$S_{3,3} = S_{6,6} = -S_{3,6} = -S_{6,3} = S,$$ (15)

where in Equations 14 and 15, S represents the value of the stiffness coefficients in tangential directions after closure. The behavior of S is assumed to represent, symbolically, the force-displacement properties as expressed by Figure 11. The stiffness coefficients in Equations 14 and 15 represent the incremental stiffness relations. The S parameter is related to the normal forces in the nodal pairs (1,2). These nodal forces have the degrees of freedom I and 4, respectively. These forces are equal and opposite. The actual calculation of the parameter S and its relation to the stresses follows the following procedure. Consider the nodal pairs (1,2). Not including the gap element, these nodal pairs will be connected to four real elements—two elements for each pairing. The special case is, of course, when nodal pairs are on the boundary, in which case, there will be only one element associated with each node. The modifications expressed by Equations 14 and 15 take affect after contact between nodal pairs has been established. During the first load steps after the contact has been established, the parameter S is chosen to be large and of the same magnitude as the modifications to stiffness coefficients corresponding to the normal directions. This procedure established that originally, after contact, no slip occurs. In the subsequent load steps, the following check for slip is followed. Using the elements in question, the computer program evaluates both normal stresses and the shear stresses in the N, T, S coordinate system. These stresses are then averaged over the four or two elements. Using the two averaged shear stresses, a resultant shear stress is calculated. The relation between the average normal stress and the average resultant shear stress is now used for checking and establishing slip conditions. The ratio between the average resultant shear and the normal stress is calculated. If this ratio is less than input value of friction coefficient, no slip is assumed to occur, and the parameter S is retained at a large value. If the stress ratio exceeds the prescribed friction coefficient, the slip will occur, and this will be achieved by reducing the stiffness parameter S to a low value. The low level of S is used to simulate the flat response in Figure 11. In the calculation, it was found that the low value of S could be

chosen to be of order of magnitude corresponding to the original gap element properties before contact. Similar procedure applies for nodal pairs (3,4). For the second orientation of the gap in the I-J coordinate system, the nodal pairs involved are (1,4) and (2,3). Similar relations are automatically calculated for this combination.

The procedure for the slip model allows for additional features. For example, it is possible to make the friction coefficient to be a function of the stresses in the N, T, S coordinate system. Also, as the slip progresses, it is possible to modify the first part of the curve of Figure 11 to be stress or deformation related. The deformation, in this case, would be specified by amount of slip that has already occurred.

4. RATE DEPENDENT PLASTICITY

4.1 Background and Objectives. One of the additional objectives of the present investigation was to introduce the theory of rate-dependent plasticity into the SAAC program (Drysdale and Zak 1983). Since the present investigation has developed a more general gap element program, SAAC2, the rate-dependent model was introduced into the SAAC2 code.

The rate-dependent model was first incorporated into the finite element formulation in connection with the SANX computer code (Zak, Craddock, and Drysdale 1979). The SANX code represents a family of related codes which has been developed for the purpose of approximate, three-dimensional finite element analysis of certain configurations. The configurations for which SANX programs were designed involve situations which have an axisymmetric appearance but have nonaxisymmetric features which render a purely axisymmetric solution inapplicable. A series of SANX programs was developed which included elastic, elastic-plastic, elastic-viscoplastic, and rate-dependent plastic material versions.

Before describing the application of the rate-dependent plasticity to the SAAC program, it is useful to review this material model and its application to incremental analysis. In its simple form, the rate-dependent plastic model can be described by the following yield function:

$$F(\sigma_{ij}, \varepsilon_{ij}^p, \dot{\varepsilon}^p) = f(S_{ij} - \alpha_{ij}) - K(\dot{\varepsilon}^p) = 0 , \tag{16}$$

14

where

$$f(S_{ij} - \alpha_{ij}) = \tfrac{1}{2}\, (S_{ij} - \alpha_{ij})\, (S_{ij} - \alpha_{ij})$$

S_{ij} = deviatoric stress

$$K = \tfrac{1}{3}\,[\,\sigma_y(\dot{\varepsilon}^p)\,]^2$$

σ_y = rate-dependent yield stress

$\dot{\varepsilon}_p = \sqrt{\tfrac{2}{3}\,\dot{\varepsilon}_{ij}^p\,\dot{\varepsilon}_{ij}^p}$, which is defined as the effective plastic strain rate

ε_{ij}^p = plastic strain

$d\alpha_{ij} = c\,d\varepsilon_{ij}^p$, where c is the constant kinematic strain hardening parameter.

The empirical relation used to define the rate-dependent yield stress is as follows:

$$\sigma_y = \sigma_0 \left[1 + b\, ln \left(1 + \frac{\dot{\varepsilon}^p}{\dot{\varepsilon}_0} \right) \right], \tag{17}$$

where

σ_0 = static yield stress

$\dot{\varepsilon}_0$ = transition strain rate

b = strain rate hardening parameter.

Using Equations 16 and 17, it is possible to develop a set of elastic-plastic, incremental stress-strain relations. These incremental stress-strain relations are then used in the finite element model. The details of obtaining the incremental stress-strain relations can be found elsewhere (Drysdale and Zak 1983) and will not be repeated here. However, it is useful to summarize the steps which lead from Equations 16 and 17 to the incremental relations. These main steps are as follows:

Step 1   During the yield process, the condition is imposed that the incremental changes satisfy the requirement that the yield function F has zero change.

Step 2   Incremental changes in plastic strain are given by the associated plastic flow rule.

Step 3   Steps 1 and 2 above yield a differential equation for the effective plastic strain.

Step 4   For each time increment, a solution of the differential equation in Step 3 is performed to obtain the effective plastic strain.

Step 5   Step 4 permits the calculation of the change of the effective plastic strain and the change in the actual plastic strain during each interval.

Step 6   Using the results of Step 5, it is then possible to write the incremental stress-strain relations.

The incremental stress-strain relations are obtained by applying Steps 1 to 6. The general form of these relations is as follows:

$$d\sigma_{ij} = A_{ijkl} d\varepsilon_{kl}$$
$$+ DE_{ijrs} \frac{\partial f}{\partial \sigma_{rs}} \frac{\partial K}{\partial \dot{\varepsilon}^p} (A - \dot{\varepsilon}^p_o)(1 - e^{-\lambda \Delta t}) , \tag{18}$$

where the parameters A_{ijkl}, E_{ijrs}, D, A, and λ are defined during the development of Equation 18. It may be noted that the right-hand side of Equation 18 forms the basis for converting the SAAC2 program to include the rate-dependent yield stress into the gap element program.

4.2 <u>Modification of the SAAC Program</u>. The rate-dependent plastic model was incorporated into the SAAC2 code. The new version of the code is called SAAC3. The changes to the SAAC2 program involved the following parts of the program: MAIN, ELPLSS, STIFF, STRESS, and TRISTF.

To create SAAC3 from SAAC2 code, it is first necessary to incorporate rate calculations. The rate calculations involve the evaluation of stress rates for each element as well as the rate of change of the effective plastic strain rate. These rates are calculated in SAAC3 by evaluating the changes of these quantities at each time or load incremental and then updating the total rates. The stress rates are needed in the calculation of the parameter A in

16

Equation 18. The rate of the effective plastic strain rate affects the derivative of K relative to $\dot{\varepsilon}^P$. The bulk of the calculations involved in the rate calculations are included in the Subroutine STRESS.

The second major change involves calculation, at each interval, of extra body forces. From Equation 18, it can be seen that the second term on the right-hand side does not contain either total incremental stress or strain. Consequently, when Equation 18 is used in the finite element model, the effect of this term is to produce terms which act as body forces. The contribution of these effective body forces is added to the incremental force matrices. This step is performed in the Subroutine TRISTF.

The actual evaluation of the second term on the right side of Equation 18 involves a number of different calculations. These calculations depend on the stress and strain rates, and they are performed in the Subroutine ELPLSS. In order to create SAAC3 from the SAAC2 code, this subroutine had to be completely rewritten. The basis for the new Subroutine ELPLSS was the SANX program with the rate-dependent yield feature. Starting with SANX, the Subroutine ELPLSS was modified and a number of changes made in the numerical calculations. These modifications corrected some numerical stability problems originally observed in the SANX program. The new version of the Subroutine ELPLSS is given in Appendix B.

The numerical instability originally observed relative to SANX program involved special loading situations. The particular load situation to which the SANX code was applied, as a test example, involved two different load cycles with step inputs. First, a uniaxial structural member was subject to a torsional load until yield occurred. After achieving yield, the structure was subjected to a constant normal strain rate load. This loading subjects the structure to a step load. The original SANX formulation led to numerical oscillations as the load was changed from torsion to uniaxial load. The new version of the Subroutine EPLSS does not have the same difficulty. In order to check the new formulation for numerical instability, a special version of SAAC3 was prepared. This version is called SAAC3X. The reason for this new version is that it simulates a constant strain rate loading. Normally, finite element programs allow for either force input or displacement boundary conditions. The

17

additional version, SAAC3X, simulates constant strain rate through displacement boundary conditions.

4.3 Input Procedure. The various gap element programs developed in this investigation have similar input procedures. The description of the input data for all these programs is similar to that needed for the original SAAC program. Appendix A gives the input procedure for the computer programs SAAC2 and SAAC3. It may be noted that the procedure for SAAC2 and SAAC3 is similar except for the fact that SAAC3 has a new input card in the beginning. This card is labelled as Card No. 0 in Appendix A. There is no difference in the input procedures for SAAC3 and SAAC3X. However, a special set of data was developed for use in connection with the special loading consisting of torsion followed by normal constant strain rate. This data was used to check numerical stability and test the previous results from the SANX code. The same results, minus the numerical instability, were achieved.

5. CODE UNIFICATION

5.1 Background. The last topic to be covered in this report involves a preliminary feasibility study involving code unification. The motivation for this study is the fact that a number of related finite element codes have been developed with similar flow charts and common parts. These programs include SAAS, SAGA, and SANX and now a new series of SAAC codes described in this report. Since these codes are similar, it is very natural to consider if they can be combined into a code with multiple functions. One aspect of this study, therefore, was involved with examining this question.

5.2 Preliminary Study. A quick review of the various codes makes it obvious that there are some easily identified common aspects. The obvious similarities are in the area of input procedure and in the fact that some of the subroutines are basically the same in all these codes. The main similarity lies in the area of generating the finite element geometrical properties. Consequently, the question which was investigated in this study was whether the geometrical portion of these codes could be separated and executed as a separate program. This was achieved by creating a truncated version of a finite element code which includes the following parts: MAIN, MESH, POINTS, MNIMX, ANGLE, and CIRCLE. This new program generates the finite element grid properties. Included is the nodal data, element information,

18

boundary conditions, and surface loads. The program does not perform any solutions since it does not create stiffness properties, matrix assembly, or solution steps. In that sense, the new program is relatively independent of any of the original codes. One application of this new code has been computer plots of finite element geometries. In this use, the code has been coupled with plotting routines, and it has been used to examine finite element grids before any solution is attempted. This application has been found to be most useful in grid generation.

Future plans in this area involve generating SAAS, SAGA, SANX, and SAAC codes without the grid generation capability and driving these with a common code similar to the one which has been developed.
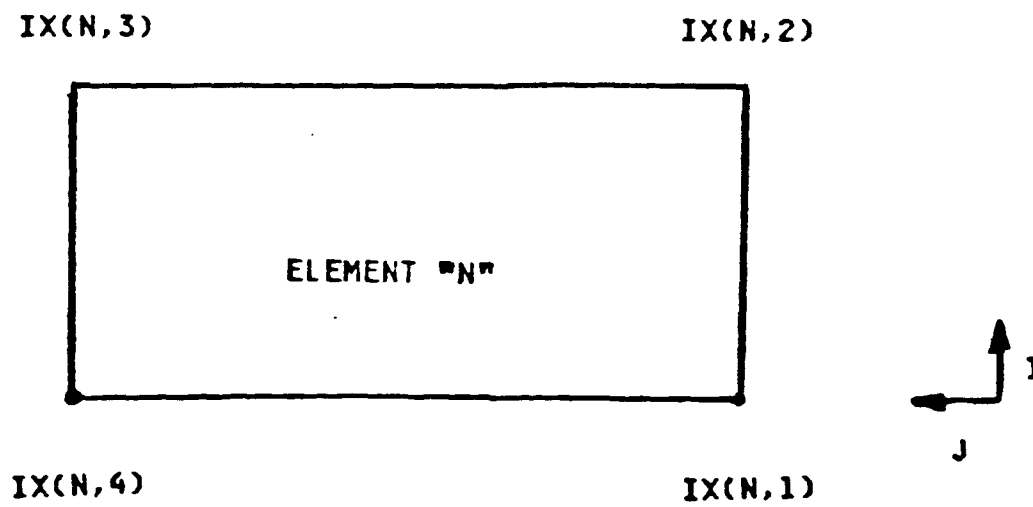
IX(N,3)   IX(N,2)

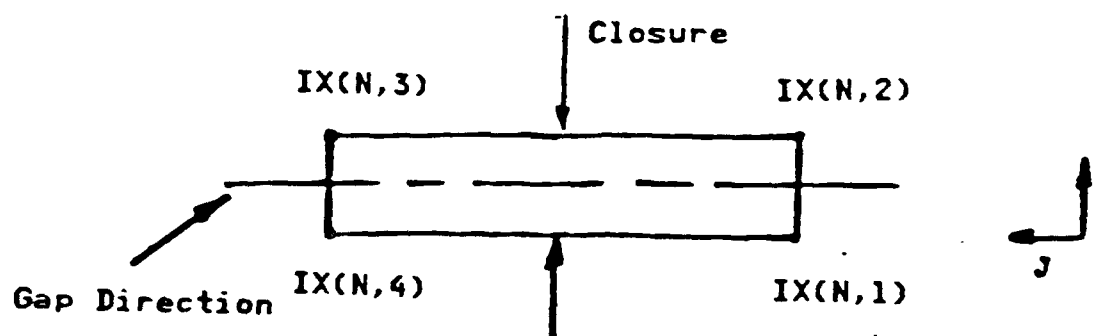ELEMENT "N"

                                                    ↑ I
                                              ←
                                               J

IX(N,4)   IX(N,1)

Figure 1. Nodal Numbering System for a Typical Element.

                            ↓ Closure
IX(N,3)   IX(N,2)

                   ↑
Gap Direction   IX(N,4)   IX(N,1)

                                                ↑ I
                                              ←
                                               J

Figure 2. Gap Element Configuration for a Gap in J Direction.

20
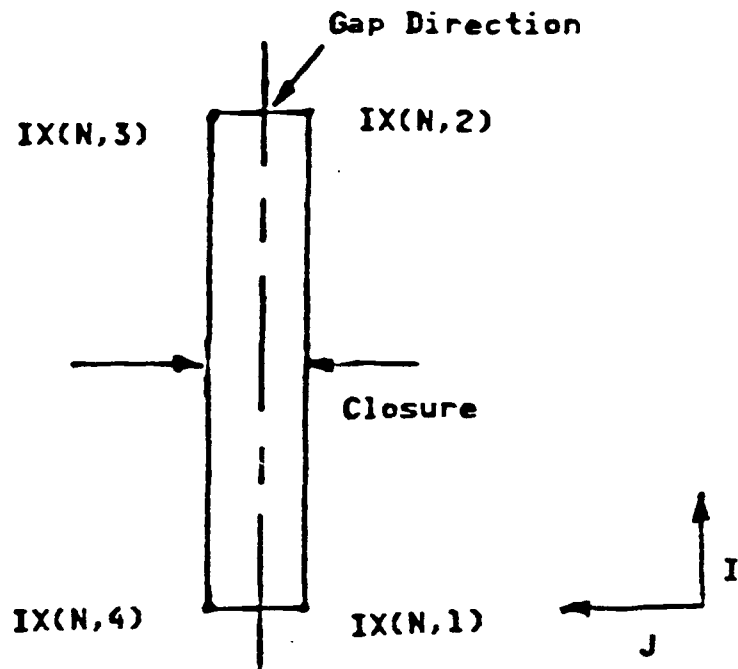
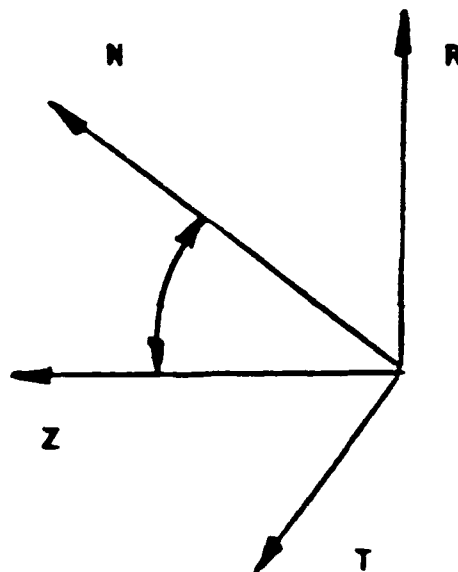Figure 3. Gap Element Configuration for a Gap in I Direction.

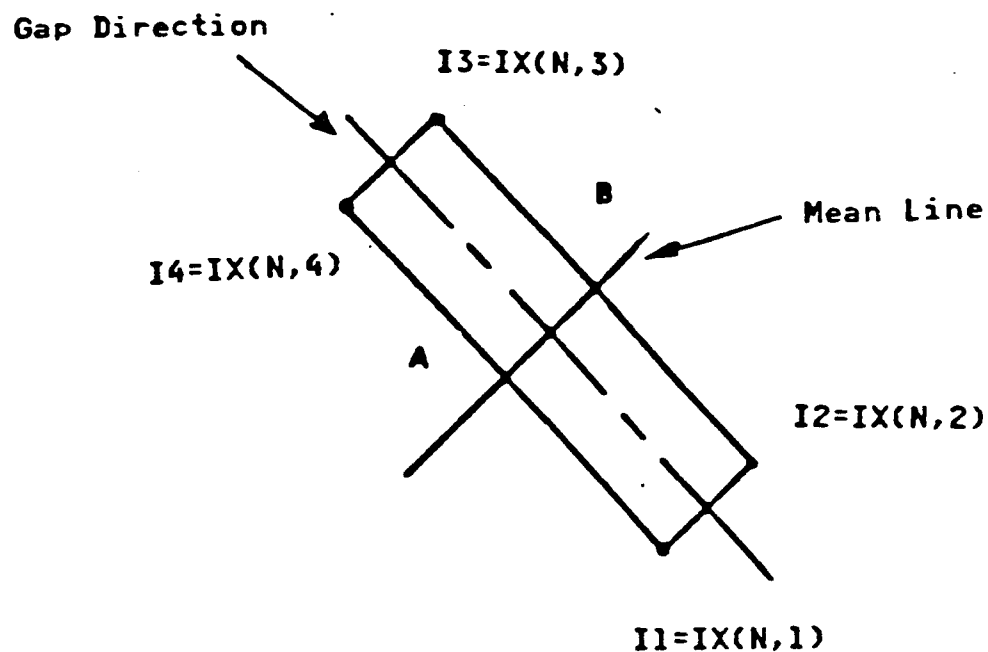Figure 4. Definition of the Gap Element Orientation Angle.

21

Gap Direction

I3=IX(N,3)

B

Mean Line

I4=IX(N,4)

A

I2=IX(N,2)

I1=IX(N,1)

Figure 5. Gap Element Mean Line Used to Determine Orientation.

IX(N,3)
7,8,9

IX(N,2)
4,5,6

ELEMENT "N"

I

J

IX(N,4)
10,11,12

IX(N,1)
1,2,3
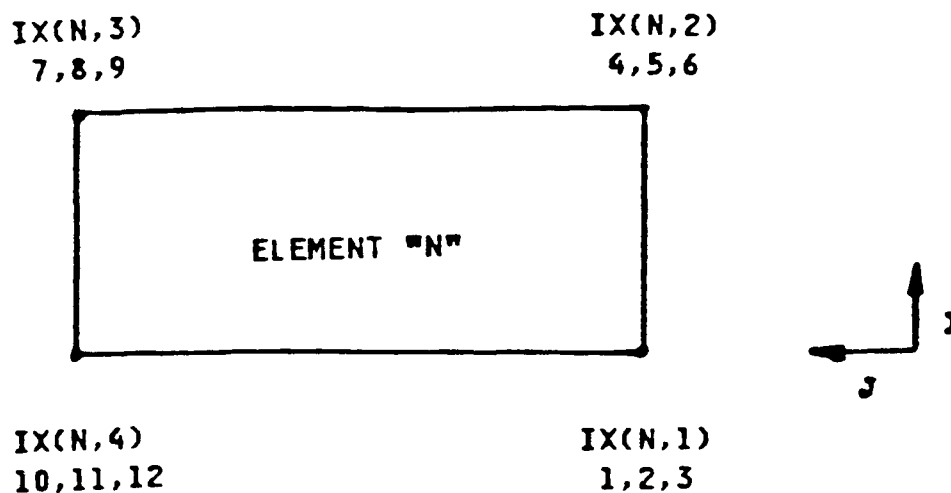
Figure 6. Degrees of Freedom for a Typical Element.

22
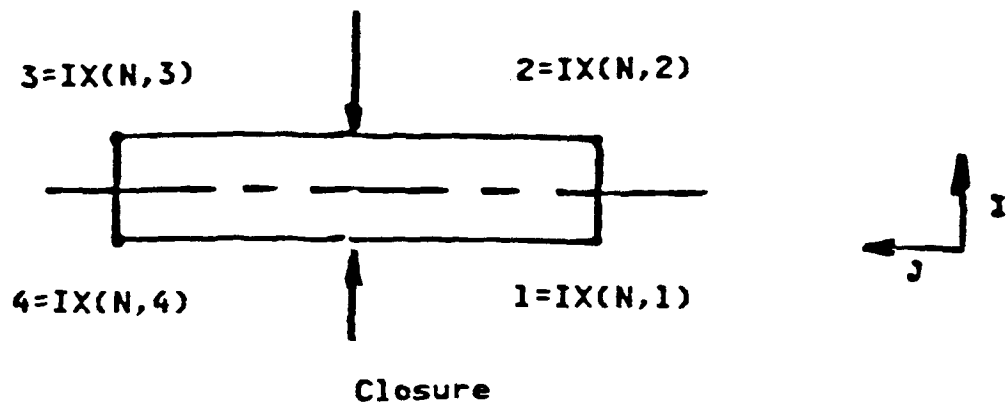
Figure 7. Gap in the J Direction Used to Illustrate Various Stiffness Modifications.

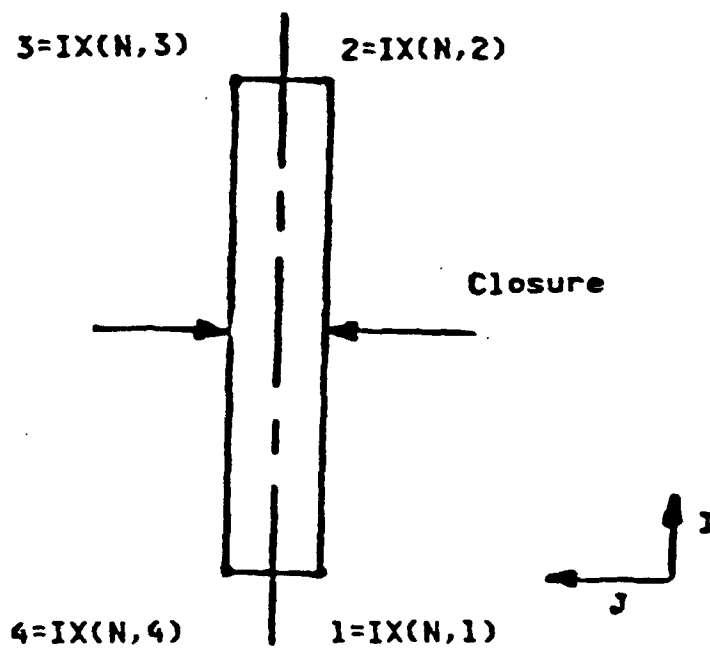Figure 8. Gap in the I Direction Used to Illustrate Various Stiffness Modifications.
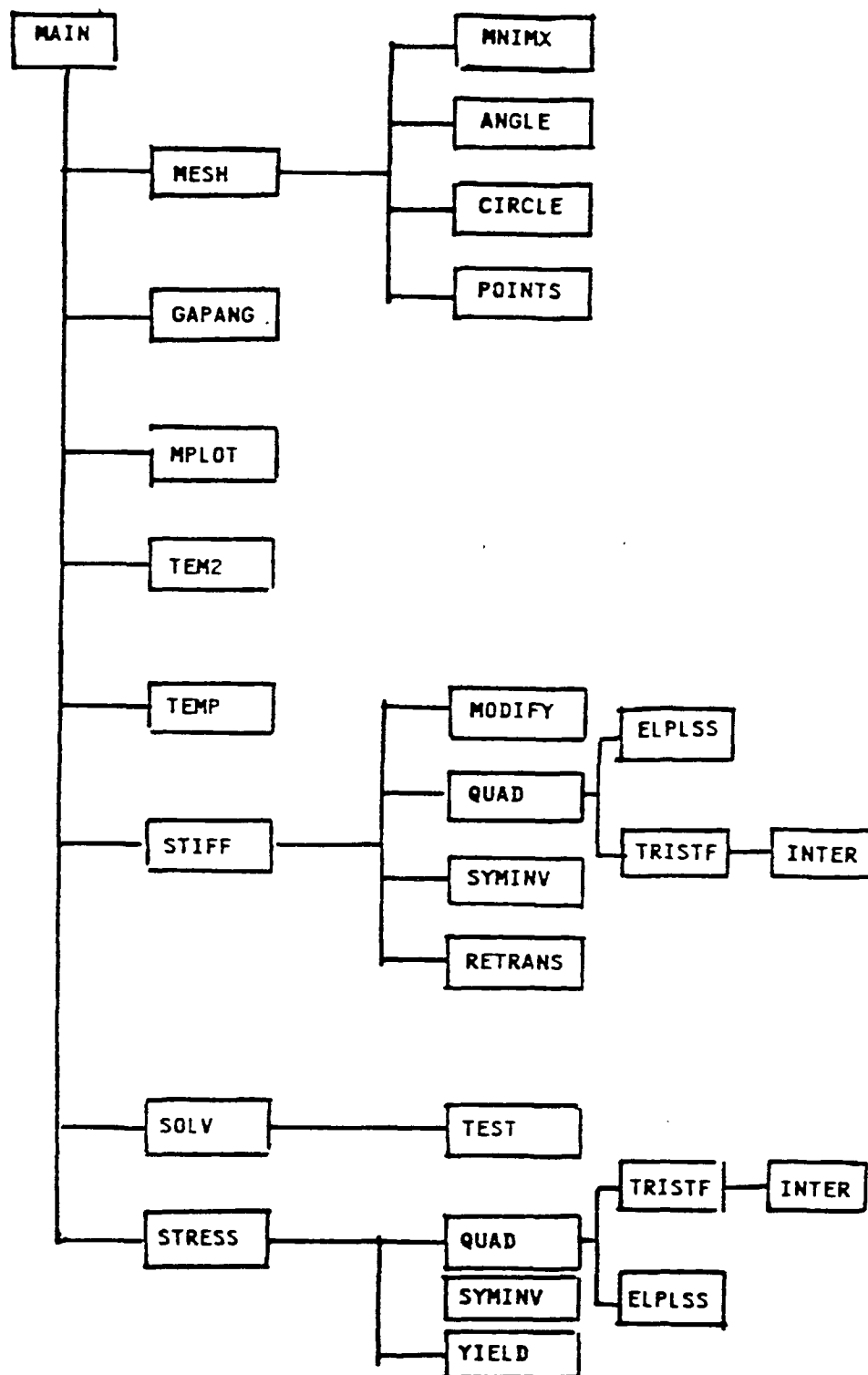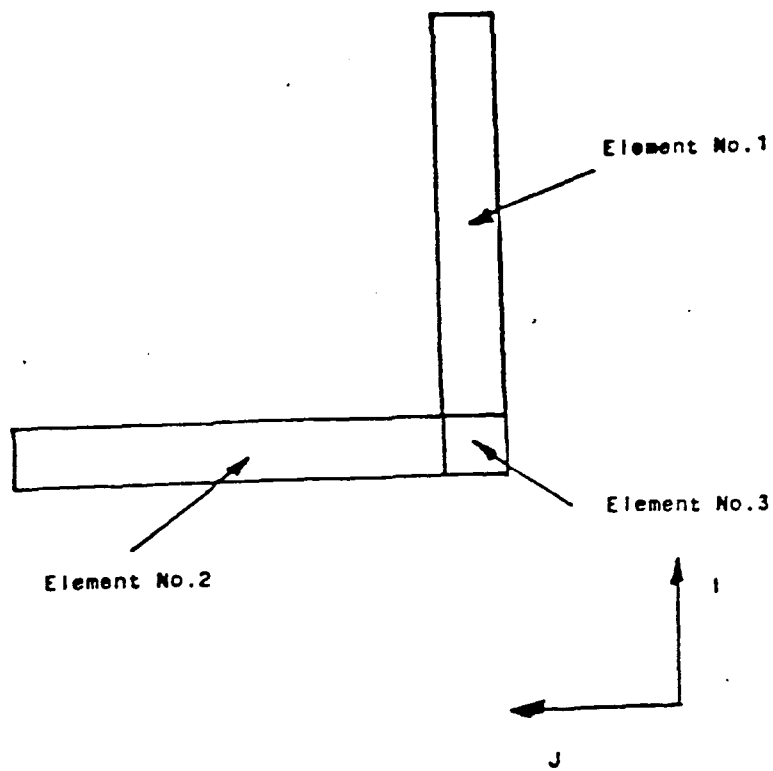
23

Figure 9. Flow Chart for SAAC Family of Codes.

Element No.1

Element No.3

Element No.2

I

J

Figure 10. <u>Generalized Gap Model</u>.
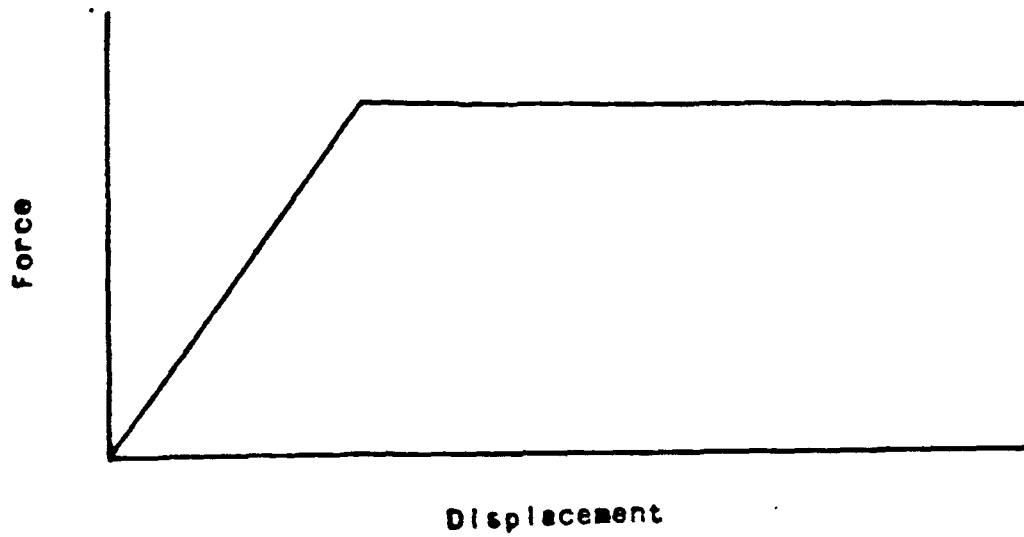
Force

Displacement

Figure 11. <u>Force-Displacement Relation for Material Slip</u>.

25

INTENTIONALLY LEFT BLANK.

6. REFERENCES

Drysdale, W. H., and A. R. Zak. "A Theory for Rate-Dependent Plasticity." International Journal of Computers and Structures, vol. 20, pp. 259–264, 1983.

Zak, A. R. "Finite Element Gap Model." Contract No. DAAK11-83-C0046, Zak Technologies Inc., Champaign, IL, November 19[.]4.

Zak, A. R., J. N. Craddock, and W. H. Drysdale. "An Elastic-Plastic Analysis of Non-Axisymmetric Structures." International Journal of Computers and Structures, vol. 10, pp. 841–846, 1979.

INTENTIONALLY LEFT BLANK.

APPENDIX A:

INPUT PROCEDURE FOR SAAC PROGRAMS

INTENTIONALLY LEFT BLANK.

DATA NO. 0 - RATE PROPERTY CARD

(Needed only for SAAC3 and SAAC3X Codes)

Format   (5E12.6)

Columns   1–12 Δt (Time increment)

                13–24   b (Rate parameter in Equation 17)

                25–36 $\dot{\varepsilon}_p$ (Rate parameter in Equation 17)

                (Next two parameters needed only for SAAC3X)

                37–48   STRRATE (Normal strain rate)

                49–60   STRSTEP (Shear stress step input)

DATA NO. 1 - TITLE CARD

Format (20A4)

Columns   1–80   Title (Title for particular case)

DATA NO. 2 - CONTROL CARD

Format (6I5, F5.0, 6I5)

Columns	1–5	NNLA (Number of nonlinear approximations; NNLA = 1 for this version of the program.)
	6–10	NUMTC (Number of temperature cards; if -2, a constant temperature is specified.)
	11–15	NUMMAT (Number of different materials; 6 maximum)
	16–20	NUMPC (Number of boundary pressure cards; 200 maximum)
	21–25	NUMSC (Number of boundary shear cards; 200 maximum)
	26–30	NUMST (Number of boundary shear cards in tangential direction; 200 maximum)
	31–35	TREF (Reference temperature)
	36–40	INERT (This parameter decides if inertia loads will be present; INERT = 0 means zero values of axial acceleration and angular acceleration and velocity for each load increment.)
	41–45	NLINC (Number of load increments with time; NLINC ≥ 1)
	46–50	INCI (If INCI = 0, then inertia loads for each time increment will be equal to the inertia load for the first time increment.)
	51–55	INCF (If INCF = 0, then surface loads for each time increment will be the same as for the first time increment.)
	56–60	IPLOT (Plot parameter; IPLOT = 1 if plot is required.)

DATA NO. 3 - MESH GENERATION CONTROL CARD

Format (5I5)

Columns	1-5	MAXI (Maximum value of I in mesh; 25 maximum)
	6-10	MAXJ (Maximum value of J in mesh; 100 maximum)
	11-15	NSEG (Number of line segment cards)
	16-20	NBC (Number of boundary condition cards)
	21-25	NMTL (Number of material block cards)

DATA NO. 4 - LINE SEGMENT CARDS

The order of line segment cards is immaterial, except when plots are requested; in this case, the line segment cards must define the perimeter of the solid continuously. The order of line segment cards defining internal straight lines is always irrelevant.

FORMAT (3[2I3, 2F8.3], I5)

Columns		
	1–3	I coordinate of the 1st point
	4–6	J coordinate of the 1st point
	7–14	R coordinate of the 1st point
	15–22	Z coordinate of the 1st point
	23–25	I coordinate of the 2nd point
	26–28	J coordinate of the 2nd point
	29–36	R coordinate of the 2nd point
	37–44	Z coordinate of the 2nd point
	45–47	I coordinate of the 3rd point
	48–50	J coordinate of the 3rd point
	51–58	R coordinate of the 3rd point
	59–66	Z coordinate of the 3rd point
	67–71	Line segment type parameter

If the number in column 71 is

0	Point (input only 1st point)
1	Straight line (input only 1st and 2nd points)
2	Straight line as an internal diagonal (input only 1st and 2nd points)

3	Circular arc specified by 1st and 3rd points at the ends of the arc and 2nd point at the midpoint of the arc
4	Circular arc specified by 1st and 2nd points at the ends of the arc with the coordinates of the center of the arc given as the 3rd point (delete I and J for 3rd point)
5	Straight line as boundary diagonal for which I of 1st point is minimum for its row and/or I of 2nd point is minimum for its row (input only 1st and 2nd points)
6	Straight line as boundary diagonal for which I of 1st point and/or 2nd point is maximum for its row (input only 1st and 2nd points)

NOTE: In specifying a circular arc, the points are ordered such that a counterclockwise direction about the center is obtained upon moving along the boundary.

DATA NO. 5 - BOUNDARY CONDITION CARDS

Each card assigns a particular boundary condition to a block of elements bounded by I1, I2, J1, and J2. For a line, I1 = I2, or J1 = J2. For a point, I1 = I2, and J1 = J2.

Format (4I5, I10, 3F10.0)

Columns	1–5	Minimum I
	6–10	Maximum I
	11–15	Minimum J
	16–20	Maximum J
	21–30	Boundary condition code
	31–40	Radial boundary condition code, XR
	41–50	Axial boundary condition, XZ
	51–60	Tangential boundary condition, XT

If the number in Columns 21–30 is

0	XR is the specified R-load,
	XZ is the specified Z-load, and
	XT is the specified θ-load.
1	XR is the specified R-displacement,
	XZ is the specified Z-load, and
	XT is the specified θ-load.
2	XR is the specified R-load,
	XZ is the specified Z-displacement, and
	XT is the specified θ-load.

3   XR is the specified R-displacement,

       XZ is the specified Z-displacement, and

       XT is the specified θ-load.

4   XR is the specified R-load,

       XZ is the specified Z-load, and

       XT is the specified θ-displacement.

5   XR is the specified R-displacement,

       XZ is the specified Z-load, and

       XT is the specified θ-displacement.

6   XR is the specified R-load,

       XZ is the specified Z-displacement, and

       XT is the specified θ-displacement.

7   XR is the specified R-displacement,

       XZ is the specified Z-displacement, and

       XT is the specified θ-displacement.

DATA NO. 6 - MATERIAL BLOCK ASSIGNMENT CARD

Each card assigns a material definition number to a block of elements defined by the I and J coordinates.

Format (5I5, 2F10.0, 2I5)

Columns		
	1–5	Material definition number (1 through 6)
	6–10	Minimum I
	11–15	Maximum I
	16–20	Minimum J
	21–25	Maximum J
	26–35	Material principal property inclination angle BETA which defines N-S plane orientation relative to z direction (see Figure 4)
	36–45	Material principal property inclination angle ALPHA which defines the orientation of the N-T plane relative to the r-z plane (see Figure 4)
	46–50	IANG (If IANG = 0, then ALPHA is same for total material block. If IANG = 1, the ALPHA varies in sign in the I direction from element to element every NANG elements. This will allow for equal but opposite helical angles.)
	51–55	NANG (Number of elements in the I direction with the same ALPHA)
	56–60	IJDIR (Gap direction 0,1, or 2)

NOTE: Gap elements will be identified by a material definition number of 2.

DATA NO. 7 - PLOT TITLE CARD

Format (20A4)

Columns   1–80   Title (Title printed under each plot)

DATA NO. 8 - PLOT GENERATION INFORMATION CARD

Format (2F10.0)

Columns   1–10   RMAX (Maximum r coordinate of mesh)

                    11–20   ZMAX (Maximum z coordinate of mesh)

NOTE: Use only if IPLOT = 1 (plot required).

DATA NO. 9 - TEMPERATURE FIELD INFORMATION CARDS

If NUMTC in columns 6-10 of the CONTROL CARD is greater than
1, the temperature field is given on cards. One card must
be supplied for each point for which a temperature is
specified.

Format (3F10.0)

Columns	1-10	R coordinate
	11-20	Z coordinate
	21-30	Temperature

If NUMTC in columns 6-10 of the CONTROL CARD is -2, a constant
temperature field is specified; the value is given on a
single card.

Format (F10.0)

Columns	1-10	Temperature

DATA NO. 10 - MATERIAL PROPERTY INFORMATION CARDS

The following group of cards must be specified for each material (maximum of 6).

a. MATERIAL IDENTIFICATION CARD

Format (2I5, 2F10.0)

Columns	1-5	Material identification number
	6-10	Number of temperatures for which properties are given (12 maximum)
	11-20	Mass density of material (if required)
	21-30	Thermal expansion parameter (If 1, free thermal expansion on the material property cards; otherwise, coefficients of thermal expansion are on the material property cards.)

b. MATERIAL PROPERTY CARDS

Two cards are required for each temperature.

First Card

Format (7F10.0)

Columns	1-10	Temperature
	11-20	Modulus of elasticity, E_N
	21-30	Modulus of elasticity, E_S
	31-40	Modulus of elasticity, E_T
	41-50	Poisson's ratio, v_{NS}
	51-60	Poisson's ratio, v_{NT}
	61-70	Poisson's ratio, v_{ST}

Second Card

Format (6F10.0)

Columns   1–10   Shear modulus, G_{NS}

               11–20   Shear modulus, G_{ST}

               21–30   Shear modulus, G_{TN}

               31–40 $\alpha_N T$ or α_N

               41–50 $\alpha_S T$ or α_S

               51–60 $\alpha_T T$ or α_T

DATA NO. 11 - YIELD STRESS CARDS

(not needed in elastic version)

Format (7F10.0)

Columns	1–10	Yield stress in tension in N direction
	11–20	Yield stress in tension in S direction
	21–30	Yield stress in tension in T direction
	31–40	Yield stress in shear in NS direction
	41–50	Yield stress in shear in NT direction
	51–60	Yield stress in shear in TS direction
	61–70	Hardening parameter; C

DATA NO. 12 - INERTIA LOAD CARD

Format (3F10.0)

Starting with this input card and including the boundary
force cards, this data is to be input as a block for
each load step, that is, NLINC times. There are the
following exceptions to this:

(a) If INERT = 0, then this card is to be
omitted completely (no inertia load).

(b) If INCI = 0, then this card is not
repeated, but appears in first block
only (the inertia loads are constant
for each load step).

(c) If INCF = 0, then the following boundary
pressure and shear cards are to be given
only for the first block and not repeated
again (the pressure and shear loads are
constants for each load increment).

Columns   1-10   ACELZ (axial acceleration)

            11-20   ANGVEL (angular velocity)

            21-30   ANGACC (angular acceleration)

DATA NO. 13 - BOUNDARY PRESSURE CARDS

One card is required for each boundary element which is subjected to a normal pressure; that is, the number of these cards is NUMPC for each load increment.

Format (2I5, F10.0)

Columns	1–5	Nodal point M
	6–10	Nodal point N
	11–20	Normal pressure

As shown in Figure A-1, the boundary element must be on the left when progressing from M to N. Surface normal tension is input as a negative pressure.
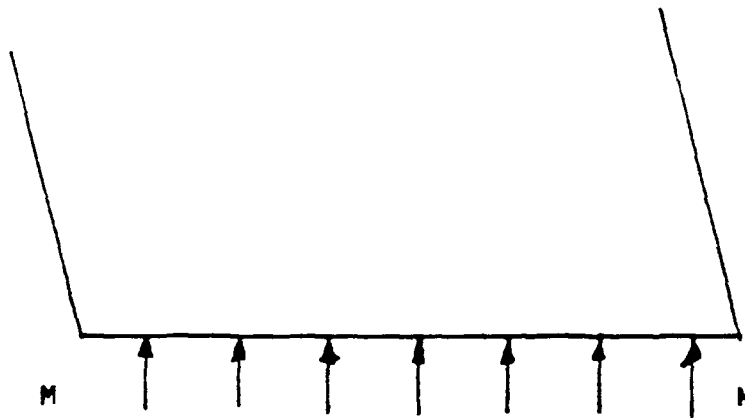
Figure A-1. Example of Boundary Pressure Loading.

DATA NO. 14 - BOUNDARY SHEAR CARDS

One card is required for each boundary element which is
subjected to surface shear; that is, the number of
these cards is NUMSC for each load increment.

Format (2I5, F10.0)

Columns	1–5	Nodal point M
	6–10	Nodal point N
	11–20	Surface shear

As shown in Figure A-2, the boundary element
must be on the left when progressing from M to N.
The positive sense of the shear is from M to N.
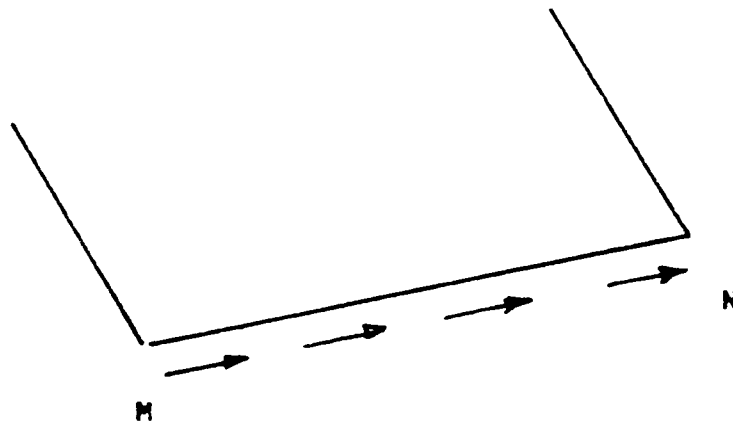
Figure A-2. Example of Boundary Shear Loading.

DATA NO. 15 - BOUNDARY TRANSVERSE SHEAR CARDS

One card is required for each boundary element which is subject to the transverse shear; that is, the number of these cards is NUMSC for each load increment.

Format (2I5, F10.0)

Columns	1–5	Nodal point M
	6–10	Nodal point N
	11–20	Surface transverse shear
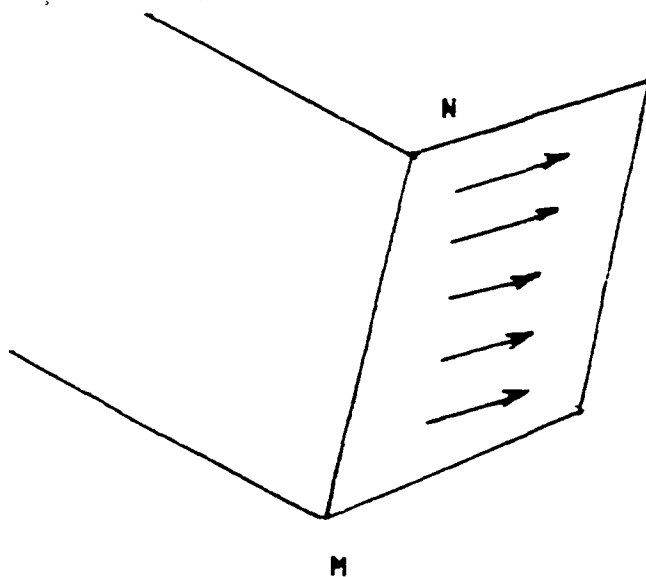
Figure A-3. Example of Boundary Transverse Shear Loading.

Intentionally left blank.

APPENDIX B:

COMPUTER LISTING OF SUBROUTINE ELPLSS

INTENTIONALLY LEFT BLANK.

```fortran
      SUBROUTINE ELPLSS(MTYPE)
      COMMON/INCR/NOL,INERT,NUMMAT,SIGTOT(12,100)
     1,EPSTOT(12,100)
      COMMON/ARG1/SIG1(18),EPS1(18),DEPSP(12),CEPSP(6,6)
      COMMON/PLAS/ALFA(6,100),SIGYLD(7,6),IFGPL(100)
      COMMON/ARG/RRR(5),ZZZ(5),RR(4),ZZ(4),S(15,15),P(15),TT(6),
     1H(6,15),CRZ(6,6),XI(10),ANGLE(4),SIG(18),EPS(18),N
      COMMON/RESULT/BS(6,15),D(6,6),C(6,6),AR,BB(6,9),CNS(6,6)
      DIMENSION DFDSIG(6),SIGYB(3),DUMM(6),D1(6,6)
C     FIND DF/DSIG
      SIGYB(1)=1./SIGYLD(1,MTYPE)**2-1./SIGYLD(2,MTYPE)**2
     1   -1./SIGYLD(3,MTYPE)**2
      SIGYB(2)=1./SIGYLD(2,MTYPE)**2-1./SIGYLD(1,MTYPE)**2
     1     -1./SIGYLD(3,MTYPE)**2
      SIGYB(3)=1./SIGYLD(3,MTYPE)**2-1./SIGYLD(2,MTYPE)**2
     1       -1./SIGYLD(1,MTYPE)**2
      DO 105 I=1,6
      SIG1(I)=SIGTOT(I+6,N)-ALFA(I,N)
105   CONTINUE
      DFDSIG(1)=2.*SIG1(1)/SIGYLD(1,MTYPE)**2+SIGYB(2)*SIG1(3)
     1 +SIGYB(3)*SIG1(2)
      DFDSIG(2)=2.*SIG1(2)/SIGYLD(2,MTYPE)**2 +SIGYB(1)*SIG1(3)
     1     +SIGYB(3)*SIG1(1)
      DFDSIG(3)=2.*SIG1(3)/SIGYLD(3,MTYPE)**2+SIGYB(1)*SIG1(2)
     1    +SIGYB(2)*SIG1(1)
      DO 110  I=4,6
110   DFDSIG(I)=2.*SIG1(I)/SIGYLD(I,MTYPE)**2
      DO 120 I=1,6
      DUMM(I)=0.0
      DO 120 J=1,6
120   DUMM(I)=DUMM(I)+CNS(I,J)*DFDSIG(J)
      D=0.
      DO 125 I=1,6
125   D=D+DFDSIG(I)*DUMM(I)
      DO 126 I=1,6
126   D=D+SIGYLD(7,MTYPE)*DFDSIG(I)**2
      D=1./D
      DO 130 I=1,6
      DO 130 J=1,6
130   D1(I,J)=DFDSIG(I)*DFDSIG(J)
      DO 140 I=1,6
      DO 140 J=1,6
      CEPSP(J,I)=0.0
      DO 140 K=1,6
140   CEPSP(J,I)=CEPSP(J,I)+D*CNS(I,K)*D1(K,J)
      DO 150 I=1,6
      DO 150 J=1,6
      D1(I,J)=0.0
      DO 150 K=1,6
150   D1(I,J) =D1(I,J)+CNS(I,K)*CEPSP(K,J)
      DO 160 I=1,6
      DO 160 J=1,6
160   CNS(I,J)=CNS(I,J)-D1(I, J)
      RETURN
      END
```

INTENTIONALLY LEFT BLANK.

2 Director
Benet Weapons Laboratory
U.S. Army Armament Research,
Development, and Engineering Center
ATTN: SMCAR-CCB,
J. Vasilakis
J. Zweig
Watervliet, NY 12189-5000

4 Commander
U.S. Army Armament Research,
Development, and Engineering Center
ATTN: SMCAR-CCH-T,
S. Musalli
SMCAR-CC,
J. Hedderich
E. Fennell
R. Price
Picatinny Arsenal, NJ 07806-5000

1 Commander
U.S. Army Armament Research,
Development, and Engineering Center
ATTN: SMCAR-TD, T. Davidson
Picatinny Arsenal, NJ 07806-5000

2 Commander
U.S. Army Materials Technology Laboratory
ATTN: SLCMT-MEC,
B. Halpin
T. Chou
Watertown, MA 02172-0001

2 Director
Lawrence Livermore National Laboratory
ATTN: S. DeTeresa
R. M. Christensen
P.O. Box 808
Livermore, CA 94550

4 Director
Sandia National Laboratories
Applied Mechanics Department,
Division-8241
ATTN: C. W. Robinson
G. A. Benedetti
K. Perano
W. Kawahara
P.O. Box 969
Livermore, CA 94550-0096

2 Battelle Pacific Northwest Laboratory
ATTN: M. Smith
M. Garnich
P.O. Box 999
Richland, WA 99352

1 Director
Los Alamos National Laboratory
ATTN: D. Rabern
WX-4 Division, Mail Stop G-787
P.O. Box 1663
Los Alamos, NM 87545

2 David Taylor Research Center
ATTN: R. Rockwell
W. Phyillaier
Bethesda, MD 20054-5000

2 Olin Corporation
Flinchbaugh Operations
200 E. High Street
ATTN: B. Stewart
E. Steiner
Red Lion, PA 17356

2 Alliant Tech Systems
5640 Smetana Drive
ATTN: J. Bode
K. Ward
Minnetonka, MN 55343

2 Project Manager
Tank Main Armament Systems
ATTN: SFAE-AR-TMA-MD,
C. Kimker
SFAE-AR-TMA-ME,
K. Russell
Picatinny Arsenal, NJ 07806-5001

1 Zak Technologies, Inc.
ATTN: Dr. Adam R. Zak
2310 Belmore Dr.
Champaign, IL 61821